

Appendix A. PEMD installation procedures in Unalaska

1. Locate anchor points on beach

- Use GPS to find requested coordinates (determined from previous oil patch positions and sample design criteria). Modify placement as necessary to sample original oil patches or adjust for topography.
- Discernable patches were generally not evident (in 2008).

2. Set supratidal anchor.

- Preference: drill bedrock or boulders; set two 13 mm anchor bolts.
 - Add 6 mm eye-eye swivel between two 13 mm washers.
 - Place two nuts at top, the upper most with a nylon bushing.
 - (All hardware was pre-cleaned; soap & water washed, dried, and sonicated in pentane.)
 - Pass groundline through both anchor points.



- Second preference: fasten groundline around large drift logs in the supratidal zone.
- Last option: set 9 kg longline anchors in supratidal.
 - These were tarred – an unfortunate circumstance – hence were used only when absolutely necessary and placed so they would not introduce PAHs into intertidal areas.
 - Tar samples were collected from anchors for hydrocarbon analysis.

3. Pass groundline to support boat (generally a 11 m landing craft, sometimes a small Zodiak).

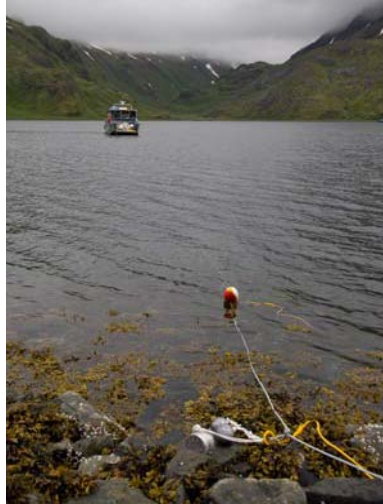
- Back boat >60 m off shore, thereby removing exhaust fumes, gas, and oil from sampling area.



4. From shore, fasten PEMD buoy string to groundline
 - Place a butterfly knot in the groundline.
 - Connect two 4.5 kg lead weights with 6 mm nylon rope (1 m long, tied with fisherman's knot) via a 8 mm shackle, 8 mm eye-eye swivel, and second 8 mm shackle.
 - Connect buoy line in second shackle; connect benthic PEMD ring (8 × 51 mm) with 6 mm nylon loop (as previous).

5. Open PEMDs; connect to float and benthic ring.

6. Drag buoy string off shore with boat to approximately 4.6 m depth.



7. Continue backing boat to pay out Danforth anchor using 10 mm polypropylene line at the back side of the anchor.
 - 8 kg anchor, with 3 m of 8 mm chain, connected to the groundline with shackles and a swivel
 - A small float marks the polypropylene tag line.

8. Pull groundline by hand from shore to set anchor.

9. Fill polyethylene net bag with about 45 kg of rock gathered intertidally near the placement site.
 - Bags were made from net (3 mm cord, 25 mm mesh, 0.9 × 1.2 m) sewn into 0.6 × 0.9 m bags with 3 mm nylon line.
 - Add a PEMD; fasten with a bowline knot in 8 mm nylon rope.
 - Place a clove hitch in groundline to close the bag.
 - Use remainder of the 8 mm rope to sew the bag closed, passing over the groundline on both sides and knotting with halt-hitches on the groundline.
 - Bag placement was approximately mid tide.



10. Tie upper end of groundline off to bolts, logs, or anchor.

11. To leave beach, land boat well downwind of samplers.

12. Allow to soak approximately 1 month.

Appendix B. Sampling comparison between oiled & reference beaches

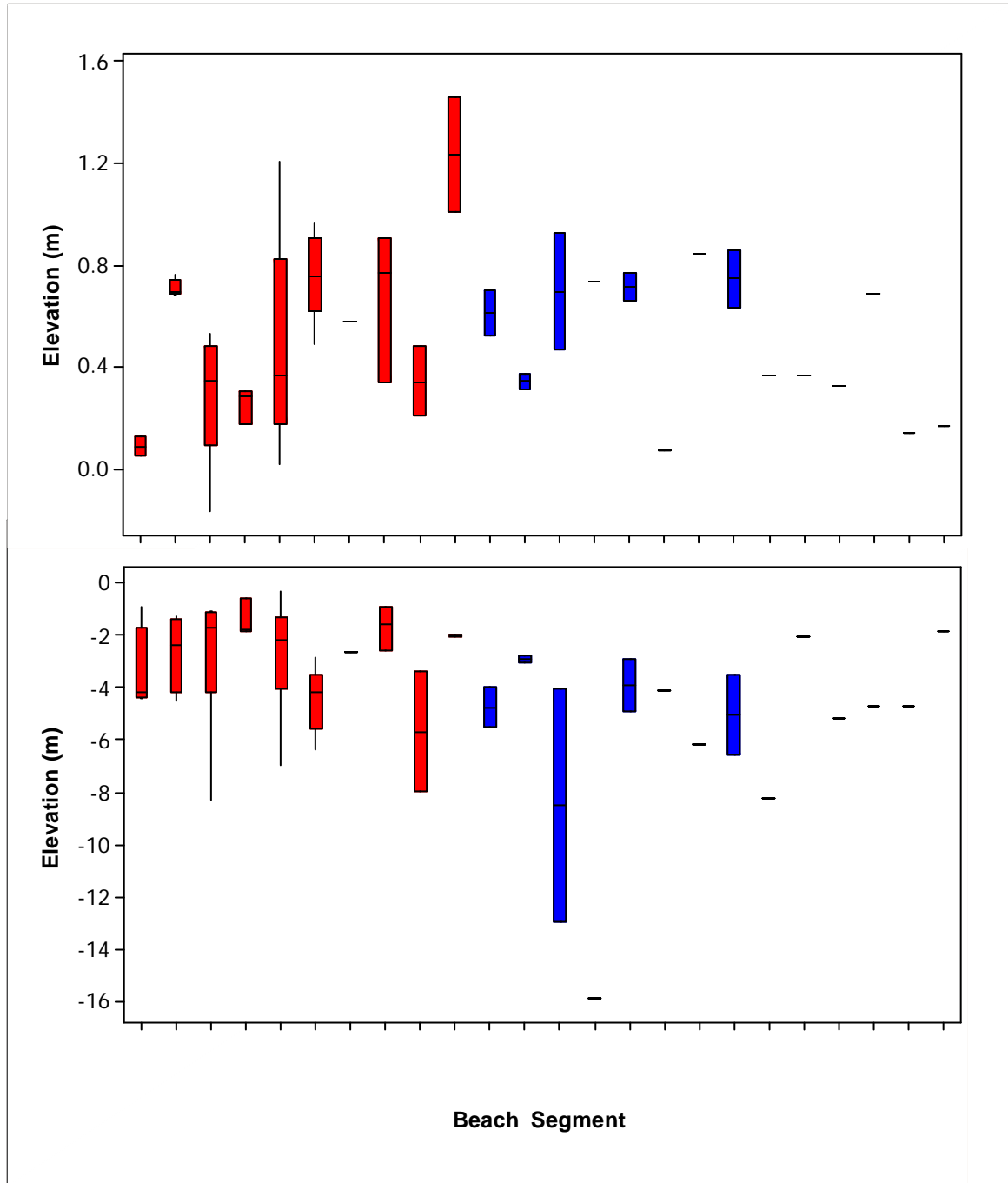
There were some minor differences and there were similarities in the way oiled and reference beaches were sampled by PEMDs. Tared longline anchors were deployed only on oiled beach segments ($n = 6$, involving 4 beach segments). The PEMD housings were buried in sediment more frequently on oiled beaches ($n = 4$ of 41) than reference beaches ($n = 1$ of 19). More importantly, only two PEMD housings were filled with sediment, both deployed in reference areas where the sediment was fine enough to pass through the 3 mm holes. Mean PEMD sample times were 30 d at all reference beach segments and 28 d (range 26 to 28 d) among oiled beach segments; sample time differed significantly [$P < 0.001$, one way ANOVA with beach segment nested in beach type (oiled or reference)].

Elevation between oiled and reference beach sections did not differ significantly ($P = 0.673$; one way ANOVA with beach segment nested in beach type). Mean intertidal PEMD elevations for all beach segments were 0.5 m; 95% confidence bounds were 0.4 to 0.6 m and the range was -0.2 to 1.5 m above or below mean lower low water (MLLW) (Fig. B1).

Mean benthic (subtidal) PEMD elevations were -5.4 and -3.0 at reference ($n = 19$) and oiled ($n = 41$) segments, respectively, and differed significantly ($P = 0.014$, one way ANOVA with beach segment nested in beach type) (Fig. A1). However, there was considerable overlap in benthic elevation between oiled and reference segments. Likewise, deployment depth varied significantly between reference and oiled segments ($P = 0.028$), a measure that does not account for tide stage.

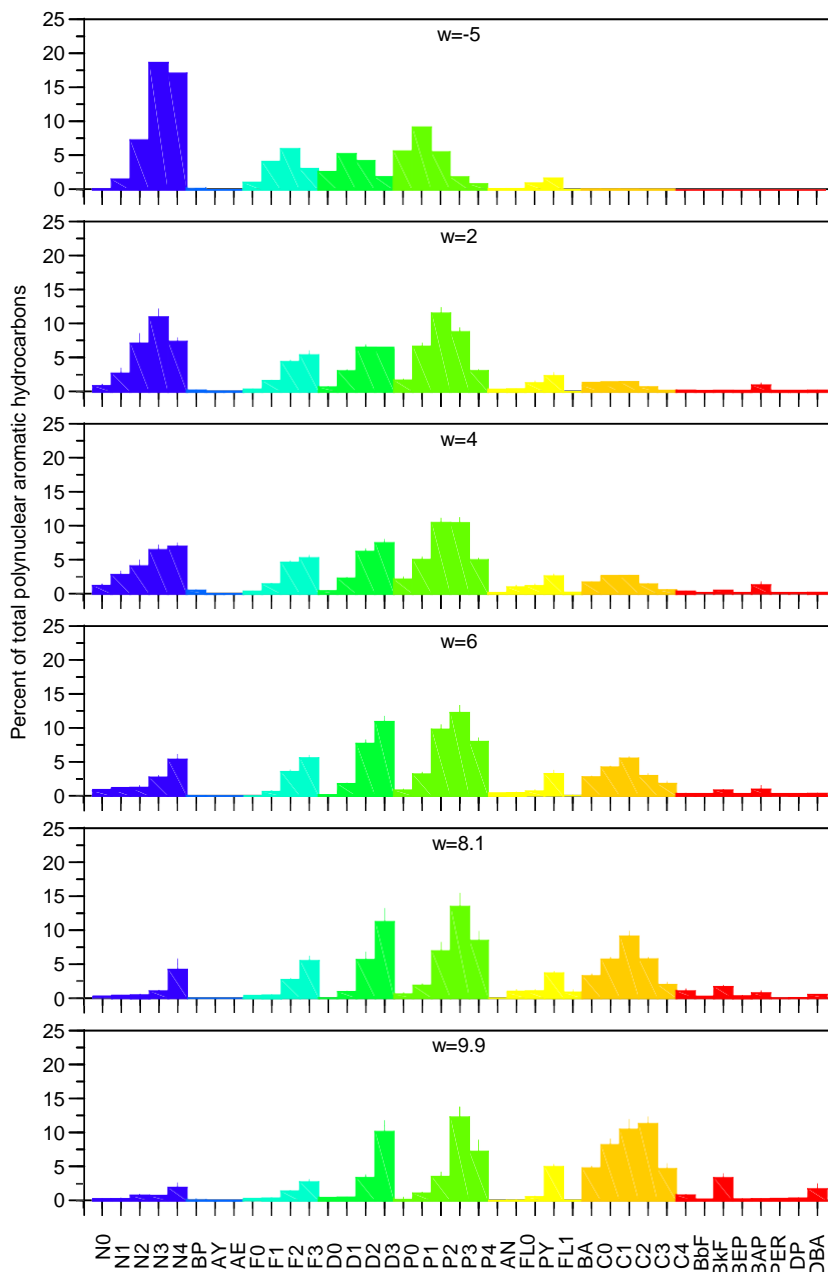
Salinity and temperature did not differ significantly between oiled and reference beaches ($P = 0.708$ and $P = 0.155$, respectively; one way ANOVA with beach segment nested in beach type). Mean salinities were 22 and 24 ppt at reference and oiled beaches; temperatures were 9.4 and 8.6 °C.

Fig. B1. PEMD elevations above or below mean lower low water (MLLW). Red box plots summarize oiled beach segments, blue box plots summarize reference segments. The top panel summarizes intertidal installations; the bottom panel summarizes subtidal (benthic) installations.



Appendix C. Brief description of PAH weathering

Weathering of PAHs describes changes in composition, from the least weathered state typically dominated by naphthalenes, to more weathered states as smaller molecular weight PAHs are preferentially lost. This process is obvious both within homologous families (e.g., naphthalenes) and among families (e.g., phenanthrenes, chrysenes) and has been summarized with a weathering index, w^1 . The following example represents sediment from Prince William Sound, Alaska, following the Exxon Valdez oil spill.



The effects of PAH weathering are to 1) progressively lose the smaller families, so that relative naphthalene concentrations, for example, become smaller while those of chrysenes, for example, become larger, and 2) the least substituted homologs within a given family are lost with time; relative phenanthrene concentrations (P0), for example become smaller with respect to substituted phenanthrenes (P3, for example). This same process has also been repeatedly observed in laboratory settings.

Understanding weathering patterns allows a better understanding of oil sources when composition of an unknown oil is compared to known source composition. In particular, the weathering coefficient, w , allows estimation of the unknown and known samples at the same weathering state¹. Several other source models have been combined with this particular approach to provide source estimates². The resultant range encompasses pyrogenic sources (negative numbers) to petrogenic sources (positive numbers). The scale of this particular model ranges from -6 to 6; values ≤ -4 are definitely pyrogenic; those ≥ 4 are definitely petrogenic. The Short and Heintz weathering model¹ was written specifically to statistically discriminate Exxon Valdez oil from other sources; it functions well in the Selendang Ayu context, though it would require fine-tuning to provide the same statistical discrimination in the latter situation.

Appendix D. Estimation of above-background concentrations

The 85th percentile tolerance interval, estimated with a 95% confidence level, was computed from the concentration distribution of reference sites to use as a threshold for judging above-background concentrations.

Explanation. A tolerance interval brackets, with a specified confidence, a particular portion of all future measurements from a distribution. For example, a one-sided upper 85% tolerance interval with 95% confidence is a threshold that is expected to only be exceeded by 15 percent (= 100% - 85%) of observations from the distribution. The confidence level refers to the probability that the interval calculated from a random sample actually will contain the expected percentage of the distribution.

Method. A statistical method published by NIST/SEMATECH was used to estimate the above-background threshold value (<http://www.itl.nist.gov/div898/handbook/prc/section2/prc263.htm>). Assuming a normal distribution, then a one-sided upper tolerance interval is calculated as

$$\bar{x} + K \cdot s$$

where \bar{x} is the estimated mean of the distribution, s is the estimated standard deviation of the distribution and K is a factor based on the sample size (n), the tolerance percentile [γ , = 0.85 as suggested by Daskalakis & O'Connor (1995)] and the confidence level (α = 0.95 for 95% confidence):

$$K = \frac{z_{1-\gamma} + \sqrt{z_{1-\gamma}^2 - ab}}{a^{1-\gamma}}, \text{ with } a = 1 - \frac{z_{1-\alpha}^2}{2(n-1)}, \quad b = z_{1-\gamma}^2 - \frac{z_{1-\alpha}^2}{n}$$

where z_p is the value that that a standard normal distribution exceeds with probability p (i.e. the p th quantile. $z_{0.95} = 1.644854$ or 1.645).

For an 85% tolerance level, with 95% confidence, ($n = 31$), the threshold formula is:

$$a = 1 - 0.0466473 = 0.9533 \text{ or about } 0.95$$

$$b = 1.074 - 0.090 = 0.984$$

$$K = (1.036 + 0.373)/0.95 = 1.483$$

Thus, the above-background threshold estimate is $\bar{x} + 1.483 \cdot s$.

Appendix E. Alkanes in mussels

Alkane concentrations in mussel tissue were typically low except pristane concentrations were often substantial (range 0 to 1194 ng/g wet weight; median was 93 ng/g). Concentrations of pristane (a biologically produced molecule) were rarely below MDL (in 3% of 105 samples). In contrast, concentrations of C15, the next most prevalent alkane, were below MDL in 38% of the samples (range 0 to 76 ng/g; median was 20 ng/g). Excluding pristane, all remaining alkanes were less than MDL in 42% of the samples; 29 to 100% of the sum of calibrated alkanes was retained in the remaining samples (mean 76%). To be consistent with PAH analysis, further comparison of alkanes in mussel tissue among areas was based on raw data (without MDL adjustment). The same conclusions are reached by examination of MDL-corrected alkanes.

Alkane composition in mussels suggests biological differences among study areas but provides little evidence of oil-related differences. For example, although the total calibrated alkane concentration was significantly greater in the oiled area than in the reference area ($P < 0.001$), pristane (a biologically produced molecule) was present in nearly every sample with detectable alkanes (98%) and it was the dominant alkane ($>50\%$ of the total mass) in 78% of the samples. Total calibrated alkane concentration minus pristane and total alkane concentration (from all sources calibrated and uncalibrated) were not significantly different among areas ($P = 0.188$ and 0.917 , respectively). The next most abundant alkane was C15; relative concentrations (normalized to the sum of calibrated alkanes) were significantly greater in Chernofski Harbor than in the reference area ($P = 0.003$) and actual concentrations were significantly greater in both Chernofski Harbor and the oiled area ($P < 0.001$). The carbon preference index (CPI) did not differ significantly among areas ($P = 0.343$; means were 1.5, 5.1, and 1.9 for reference Chernofski Harbor, and the oiled area, respectively). Normalized low molecular weight alkane ($\leq C17$) values were significantly greater in Chernofski Harbor than in the reference area ($P < 0.001$; means were 7, 32, and 19%). Normalized high molecular weight alkane values ($\geq C27$) were highest in the reference area ($P = 0.017$; means were 9, 6, and 1%). Mid and high molecular weight alkanes were typically odd, consistent with plant origins. No area-specific overall alkane composition patterns were evident, whether classified by hand or by PCA.

Geographic distributions of the two dominant alkanes in mussel tissue were roughly inverses. Pristane was not distributed evenly within areas; concentrations were consistently greatest along the kelp-bed area stretching from KFP01 to SKN05 (Fig. alk1). Pristane concentrations were greater at the mouth of Pumicestone Bay than within. Humpback Bay was the pristane hotspot within Makushin Bay. In contrast, C15 alkane concentrations were generally greatest where pristane concentrations were relatively small (Chernofski Harbor, southern Skan Bay, and Portage Bay; Fig. alk2). However, some C15 alkane concentrations were high in Humpback Bay, coincident with high pristane concentrations, and C15 concentrations were small in Pumicestone Bay, coincident with relatively low pristane concentrations Fig. alk2.

Fig. alk1. Pristane concentrations in mussel tissue, summer 2008. <musPristane.mxd>

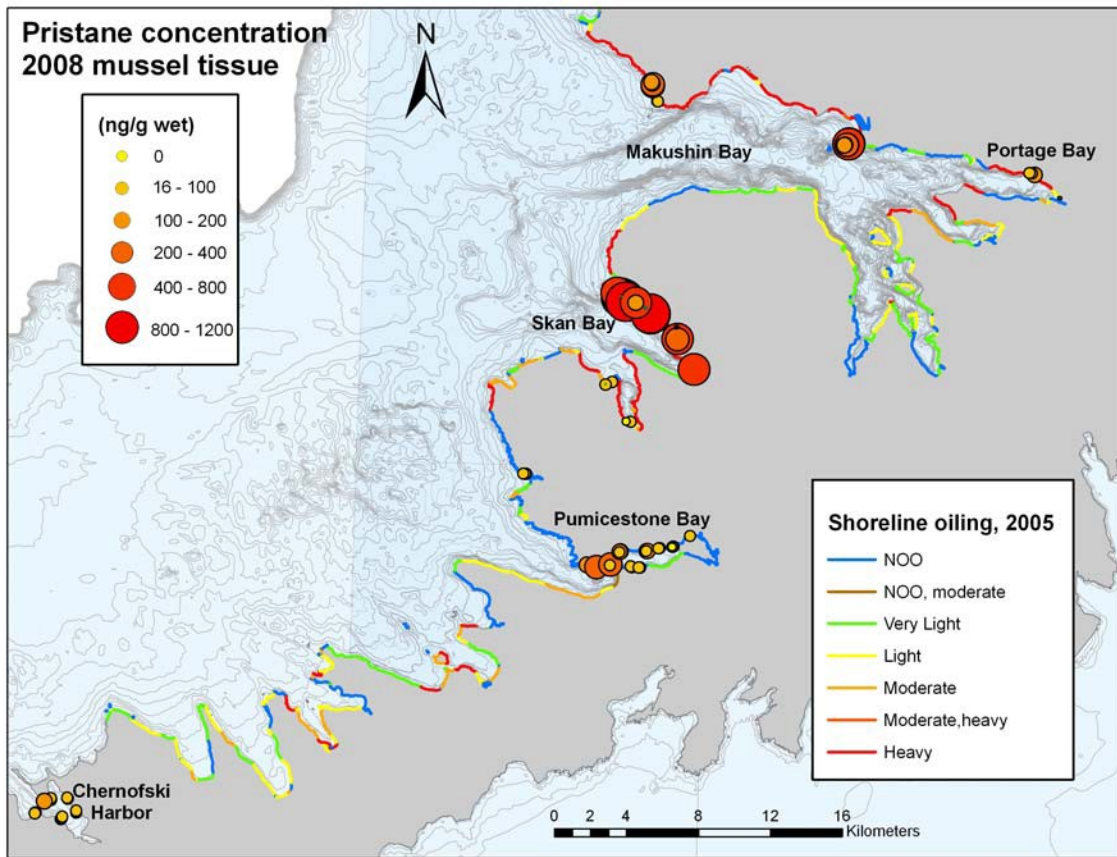
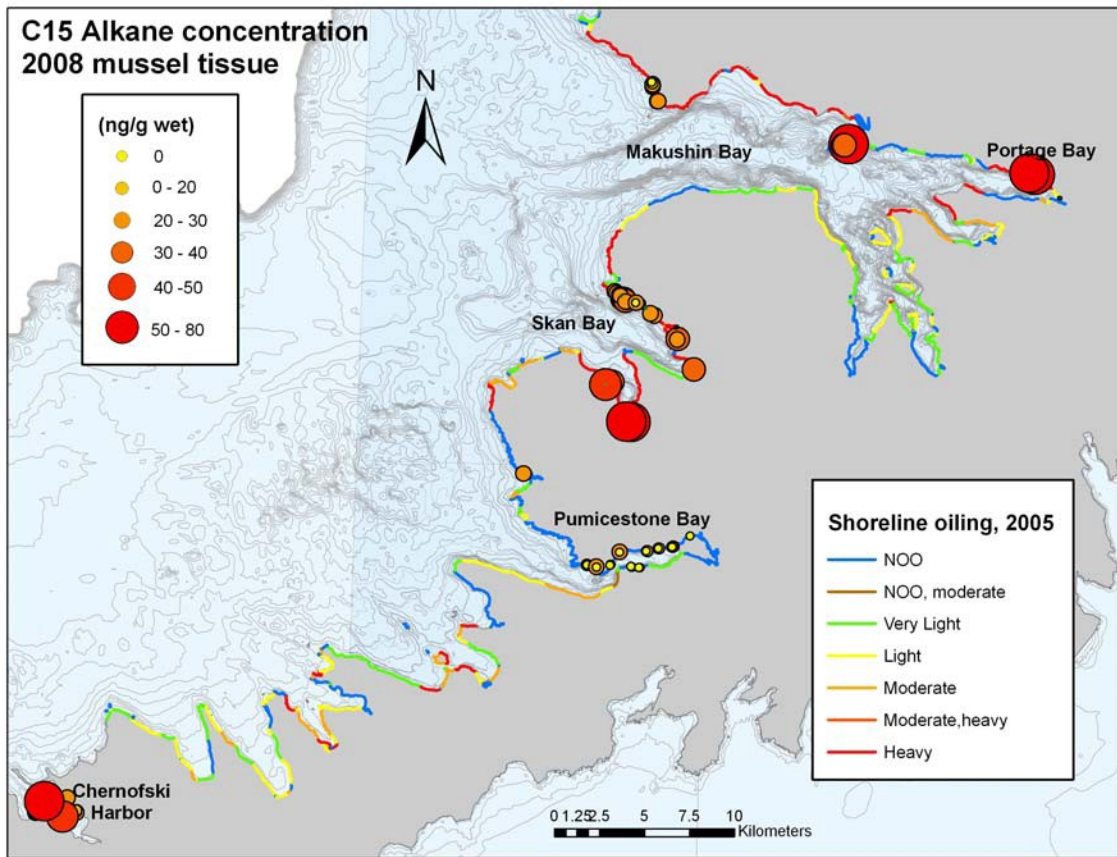
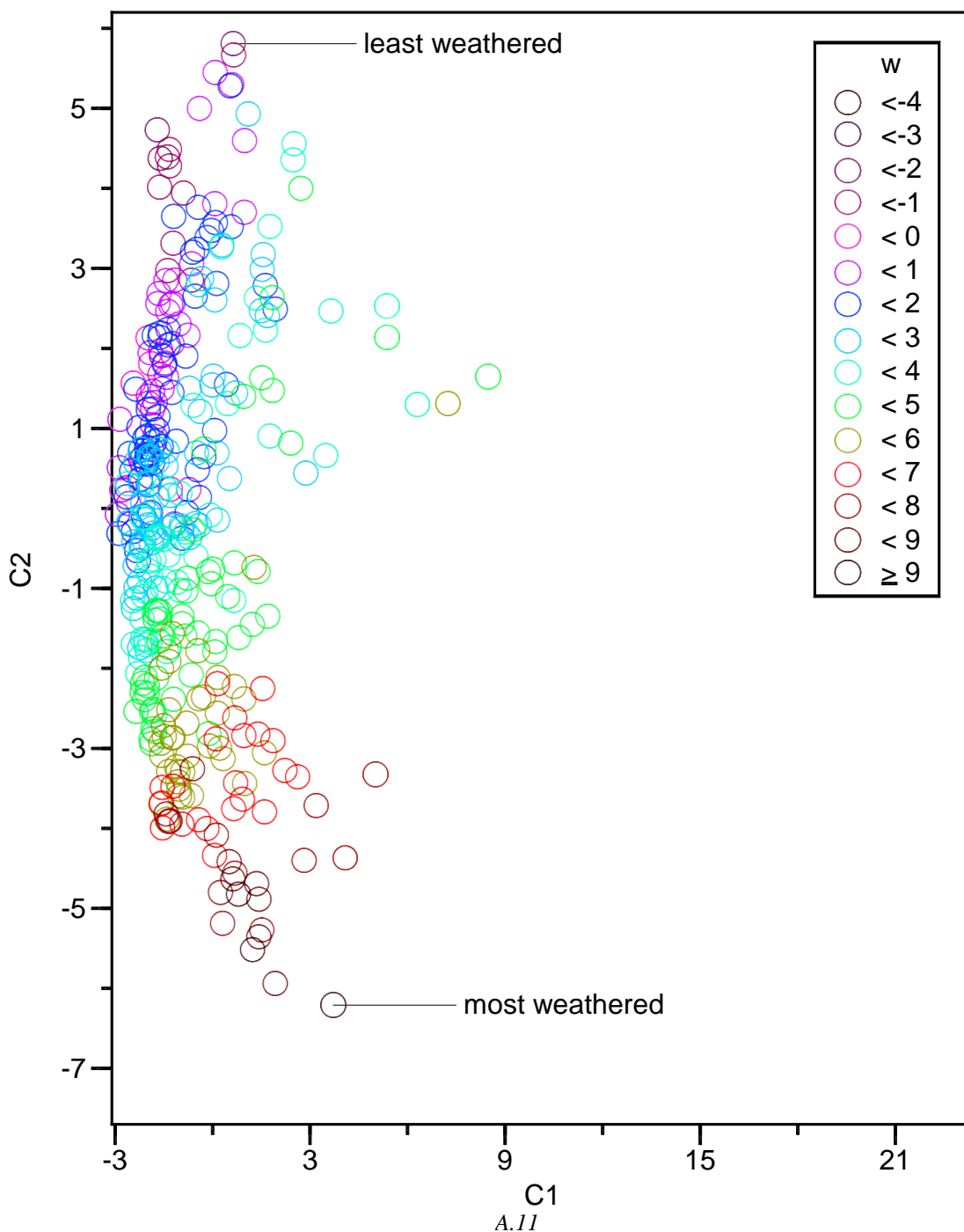


Fig. alk-2. C15-alkane concentration in mussel tissue, summer 2008. <musC15.mxd>



Appendix F. Relationship between weathering and principal components in Prince William Sound sediment

These data from Prince William Sound are included for comparison with *Selendang Ayu* oil samples, both analyzed with Principal Components Analysis. Below are the first and second principal components from the correlation matrix of normalized PAHs in oiled Prince William Sound sediment samples (1989 to 2000) where model results identified *Exxon Valdez* oil¹ color coded by weathering coefficient (w). The same basic relationship emerged in both data sets; w was correlated with the principal components, explaining the distribution illustrated below.



References

1. Short, J. W.; Heintz, R. A., Identification of *Exxon Valdez* oil in sediments and tissues from Prince William Sound and the northwestern Gulf of Alaska based on a PAH weathering model. *Environmental Science and Technology* 1997, 31, (8), 2375-2384.
2. Carls, M. G., Nonparametric identification of petrogenic and pyrogenic hydrocarbons in aquatic ecosystems. *Environmental Science & Technology* 2006, 40, (13), 4233-4239.